

# Journal of Materials Chemistry B

Accepted Manuscript



This is an *Accepted Manuscript*, which has been through the RSC Publishing peer review process and has been accepted for publication.

*Accepted Manuscripts* are published online shortly after acceptance, which is prior to technical editing, formatting and proof reading. This free service from RSC Publishing allows authors to make their results available to the community, in citable form, before publication of the edited article. This *Accepted Manuscript* will be replaced by the edited and formatted *Advance Article* as soon as this is available.

To cite this manuscript please use its permanent Digital Object Identifier (DOI®), which is identical for all formats of publication.

More information about *Accepted Manuscripts* can be found in the [Information for Authors](#).

Please note that technical editing may introduce minor changes to the text and/or graphics contained in the manuscript submitted by the author(s) which may alter content, and that the standard [Terms & Conditions](#) and the [ethical guidelines](#) that apply to the journal are still applicable. In no event shall the RSC be held responsible for any errors or omissions in these *Accepted Manuscript* manuscripts or any consequences arising from the use of any information contained in them.

1 **Guanidinium Functionalized Superparamagnetic Silica**  
2 **Spheres for Selective Enrichment of Phosphopeptides and**  
3 **Intact Phosphoproteins from Complex Mixtures**  
4

5 Qiliang Deng<sup>1,2</sup>, Jianhua Wu<sup>2</sup>, Yang Chen<sup>1</sup>, Zhijun Zhang<sup>2</sup>, Yang Wang<sup>2</sup>, Guozhen  
6 Fang<sup>2</sup>, Shuo Wang<sup>2\*</sup> and Yukui Zhang<sup>3</sup>

7  
8  
9 <sup>1</sup> Department of Science, Tianjin University of Science and Technology, Tianjin  
10 300457, P.R.China

11 <sup>2</sup> Key Laboratory of Food Nutrition and Safety, Ministry of Education of China,  
12 Tianjin University of Science and Technology, Tianjin 300457, P.R.China

13 <sup>3</sup> Key Laboratory of Separation Science for Analytical Chemistry, Dalian Institute  
14 of Chemical Physics, Chinese Academic of Sciences, DaLian, 116023, P.R.China.

---

\*Corresponding author. Tel: (+86 22)60601456; Fax: (+86 22)60601332; Email: S.wang@tust.edu.cn

15 **ABSTRACT**

16 Phosphorylation of protein regulates nearly all biological processes in nature.  
17 The development of enrichment technique for phosphorylated proteins is vital to  
18 systematic identification and characterization of phosphoproteins. Here, a general  
19 strategy for highly efficient capture of intact phosphorylated proteins from protein  
20 mixtures has been developed by using guanidine functionalized superparamagnetic  
21 microspheres (denoted as  $\text{Fe}_3\text{O}_4@\text{SiO}_2@\text{GDN}$ ). The  $\text{Fe}_3\text{O}_4@\text{SiO}_2@\text{GDN}$  was  
22 prepared by modifying  $\text{Fe}_3\text{O}_4@\text{SiO}_2$  with 3-guanidopropyl triethoxysilane as  
23 functionalization monomer. The resulting materials could specifically and selectively  
24 recognize phosphoproteins, and showed high binding capacities for model  
25 phosphoproteins ( $78.8\text{mg g}^{-1}$  for ovalbumin (OVA) and  $59.6\text{mg g}^{-1}$  for  $\beta$ -Casein  
26 ( $\beta$ -Cas), respectively). The feasibility of the resulting material for phosphoproteins  
27 enrichment has also been demonstrated by selectively binding and capturing  
28 phosphoproteins from complex protein mixtures and real samples (milk, egg, and  
29 tissue protein extract from mouse liver), respectively. In addition, the selective  
30 enrichment of phosphopeptides has also been investigated. The proposed technique  
31 showed application potential for phosphoproteins and phosphopeptides enrichment.

32

33 **Keywords:** Guanidine; phosphoproteins enrichment; proteomic; superparamagnetic  
34 microspheres

35

## 36 **1. Introduction**

37 Phosphorylation of protein is one of the most important and dynamic  
38 post-translational modifications in nature, which regulates nearly all biological  
39 processes, including signal transduction, homeostasis, apoptosis, proliferation,  
40 transcriptional and translational regulation.<sup>1-2</sup> Dysregulation of protein  
41 phosphorylation has been linked to numerous serious diseases such as cancer and  
42 diabetes. Systematic identification and characterization of phosphoprotein is vital to  
43 help us understand this important modification; however, it remains a challenging task  
44 due to the relatively low abundance of phosphorylated proteins in biological  
45 samples.<sup>3-5</sup> Current approaches to capture phosphoproteins generally rely on the  
46 interaction of phosphate anions with metal ions, such as in immobilized metal affinity  
47 chromatography (IMAC) and in metal oxide affinity chromatography (MOAC).<sup>6-10</sup>  
48 Even though these techniques have been demonstrated with success to a certain extent,  
49 some disadvantages are encountered with these techniques: including poor selectivity,  
50 low adsorption efficiency and significant losses of phosphorylated proteins during the  
51 wash steps.<sup>11-12</sup>

52 Herein, we propose a general strategy for high efficient capture of intact  
53 phosphorylated proteins from protein mixtures based on interaction between  
54 phosphate groups and guanidine groups. Guanidinium group has a pKa of 13.6 and  
55 normally possesses a delocalized positive charge which is distributed over all three  
56 nitrogen atoms over a wide pH range. It has a flat and trigonal arrangement in which  
57 two protons are oriented roughly the same direction and can stabilize two parallel

58 hydrogen bonds. Because of strong ability to bind anions through hydrogen bonding  
59 and charge pairing interactions developing guanidinium-based artificial receptors for  
60 the purpose of anions recognition has attracted much attention.<sup>13-14</sup> In nature,  
61 enzymes often bind anionic substrates by using the guanidinium-containing side chain  
62 of arginine in their active sites.<sup>15-17</sup> On the other hand, the acid dissociation constant  
63 of phosphate groups is roughly  $pK_{a1}=2.12$  and  $pK_{a2}=7.21$ , respectively. The  
64 geometric arrangement of this functional group is tetrahedral about the phosphorus, in  
65 which the O-P-O bond angles are roughly  $109.5^\circ$  and three equivalent oxygen atoms  
66 share one or two negative charges. Thus the arrangement of phosphate group is  
67 favorable for its interaction with guanidinium group. Recently, wood et al. reported  
68 that the guanidinium group of arginine formed a more stable interaction with the  
69 phosphate group than adjacent carboxyl group from Asp or Glu. The electrostatic  
70 interaction of the arginine-phosphate exhibits “an amazing covalent-like”  
71 stability.<sup>18-19</sup> However, to the best of our knowledge, the approach for phosphoprotein  
72 enrichment based on the guanidinium functionalized receptor has not been exploited  
73 previously.  
74 In this research, guanidinium functionalized superparamagnetic silica spheres  
75 (denoted as  $Fe_3O_4@SiO_2@GDN$ ) were prepared by using superparamagnetic  $Fe_3O_4$  as  
76 core due to the facile isolation and without retaining residual magnetism after removal  
77 of the external magnetic field. The recognition properties of the resulting materials for  
78 intact phosphorylation proteins were investigated by using  $\beta$ -casein ( $\beta$ -Cas, molecular  
79 weight (MW) 24kDa, isoelectric point (pI) 4.6~5.1) and ovalbumin (OVA, MW  
80 45kDa, pI 4.7) as model phosphoproteins, and bovine serum albumin (BSA, MW

81 67.0kDa, pI 4.8), hemoglobin (Hb, MW 65.0 kDa, pI 6.9 ) trypsin (Try, MW 10.5  
82 kDa, pI 10.0), Myoglobin (Mb, MW 16.7, pI 6.99 ), Lysozyme (Lyz, MW 14.0 kDa,  
83 pI 11.0 ) and Cytochrome C (Cyc, MW 12.4 kDa, pI 9.8), as non-phosphorylated  
84 proteins, respectively. Further, the resulting material has also been evaluated for the  
85 enrichment of intact phosphoproteins from complex real samples (milk, egg, and  
86 tissue protein extract from mouse liver). The schematic diagram was shown in Figure  
87 1.

## 88 2. Experimental

### 89 2.1 Materials and reagents

90  $\gamma$ -Aminopropyl triethoxysilane ( $\gamma$ -APS), 3-(2-aminoethylamino) propyltriethoxysilane,  
91 2-ethyl-2-thiopseudourea hydrobromide and tetraethylorthosilicate (TEOS) were all  
92 obtained from TCI (Shanghai, China). Tris(hydroxymethyl) aminomethane (Tris),  
93 3-(N-morpholino) propanesulfonic acid (MOPS) and  
94 4-(2-Hydroxyethyl)-1-piperazineethane sulfonic acid (HEPES) were all purchased  
95 from Alfa Aesar (Beijing, China). DL-Dithiothreitol (DTT), iodoacetamide (IAA),  
96 3-[(3-Cholamidopropyl)dimethylammonio] propanesulfonate (CHAPS), sodium  
97 orthovanadate ( $\text{Na}_3\text{VO}_4 \cdot 12\text{H}_2\text{O}$ ), sodium fluoride (NaF), ammonium bicarbonate,  
98 phenylmethanesulfonyl fluoride (PMSF), ethyleneglycol-bis(2-aminoethylether)-  
99 N,N,N',N'-tetraacetic acid (EGTA), glacial acetic acid, sodium acetate anhydrous  
100 were all obtained from J&K Scientific Ltd. (Beijing, China). Trifluoroacetic acid  
101 (TFA) were purchased from Merck (Darmstadt, Germany). Trypsin from bovine  
102 pancreas TPCK treated and  $\beta$ -Cas was purchased from Sigma-Aldrich (St., Louis,  
103 MO). All other proteins were obtained from Shanghai Sangon BioTech (Shanghai,  
104 China). Fresh milk and egg were purchased from a local supermarket. Adult female  
105 C57 mice were purchased from Laboratory Animal Center of Academy of Military

106 Medical Sciences (Beijing, China). All aqueous solutions were prepared in doubly  
107 deionized water (DDW, 18.2 M $\Omega$  cm<sup>-1</sup>) from a Millipore water purification system  
108 (Millipore, Billerica, MA, USA). Pro-Q<sup>®</sup> Diamond phosphoprotein gel staining was  
109 obtained from life technologies corporation (Invitrogen, China).

## 110 **2.2 Instruments**

111 FT-IR spectra (4000-400 cm<sup>-1</sup>) in KBr were performed on a Vector 22 spectrometer  
112 (Bruker, Germany). <sup>1</sup>H NMR spectra were recorded with a Bruker AVIII spectrometer  
113 (Bruker, Germany). Scanning electron microscope (SEM) images were obtained with  
114 a Hitachi SU-1510 (Hitachi, Japan). Transmission electron microscope (TEM) and  
115 energy dispersive X-ray analysis (EDAX) were carried out on a JEM-2100 TEM  
116 (JEOL, Japan). The magnetic property of the ferrite microsphere was investigated  
117 with a vibrating sample magnetometer (VSM) (Quantum Design, USA). Thermo  
118 gravimetric analysis (TGA) was obtained from SDTQ600 (TA, USA) at a heating rate  
119 of 10 °C min<sup>-1</sup> up to 800 °C. X-ray photoelectron spectroscopy analysis (XPS)  
120 experiment was carried out on a XPS PHI1500VersProbe (ULVAC-PHI, Japan).  
121 Micropore size and surface area were detected on a AUTOSORB-1-MP  
122 (Quantachrome, USA). The obtained gels were observed on Imagequant TM Las4000  
123 (GE, USA) and Gel Doc<sup>TM</sup> XR (Bio-Rads, USA), respectively. All MALDI-TOF  
124 mass spectra were obtained on a Bruker FLEX<sup>TM</sup> time of flight mass spectrometer  
125 (Bruker, Bremen, Germany).

## 126 **2.3 Synthesis of 3-guanidopropyl triethoxysilane**

127 2-Ethyl-2-thiopseudourea hydrobromide (3.5 g, 18.9 mmol) was dissolved in a  
128 mixture of 3.0 mL of dimethyl sulphoxide (DMSO) and 3.5 mL of and  
129 tetrahydrofuran (THF). After magnetic stirring for 20 min,  $\gamma$ -APS (4.45 mL, 19 mmol)  
130 was dropped slowly at 0 °C. The mixture was then maintained for 48 h under stirring

131 at 25 °C. After removal of DMSO and THF, the viscous transparent liquid was  
132 obtained, and characterized by FT-IR and  $^1\text{H}$  NMR, respectively. The results were  
133 shown as following: FT-IR (KBr), 3338, 3162, 2975, 2929, 2890, 1668, 1436, 1313,  
134  $1076\text{cm}^{-1}$ ;  $^1\text{H}$  NMR (400 MHz,  $\text{DMSO-}d_6$ ),  $\delta = 7.095$  (br.s, 4H, NH's), 3.746 (m, 6H,  
135 O- $\text{CH}_2$ -C), 3.109 (m, 2H, N- $\text{CH}_2$ -C), 1.563 (m, 2H, C- $\text{CH}_2$ -C); 1.140 (m 9H, C- $\text{CH}_3$ );  
136 0.574( q, 2H, Si- $\text{CH}_2$ -C).

#### 137 **2.4 Preparation of superparamagnetic $\text{Fe}_3\text{O}_4@SiO_2$ microspheres**

138 Magnetic microspheres with an average diameter of 200 nm were synthesized by a  
139 solvothermal reduction method.<sup>20</sup> In detail,  $\text{FeCl}_3 \cdot 6\text{H}_2\text{O}$  (2.7 g, 10 mmol) was  
140 dissolved in ethylene glycol (80.0 mL), and then anhydrous sodium acetate (7.2 g)  
141 and polyethylene glycol (2.0 mL) were also added. The mixture was first stirred with  
142 a magnetic stirring bar for 30 min, and then poured into a Teflon lined stainless-steel  
143 autoclave (100.0 mL). The autoclave was maintained at 200 °C for 8 h. After cooling  
144 to room temperature, the  $\text{Fe}_3\text{O}_4$  microspheres were washed with ethanol three times,  
145 and dried in a vacuum oven at 60 °C for 6 h. Subsequently, the  $\text{Fe}_3\text{O}_4$  microspheres  
146 were coated with TEOS by a modified sol-gel technique.<sup>21</sup> In detail,  $\text{Fe}_3\text{O}_4$   
147 microspheres (400.0 mg) were dispersed into toluene (100.0 mL) under  
148 ultrasonication. TEOS (3.0 mL) and triethylamine (3.0 mL) were then added into the  
149 mixtures in sequence. The mixtures were stirred at room temperature for 24 h. The  
150 resulting  $\text{Fe}_3\text{O}_4@SiO_2$  microspheres were collected and washed with ethanol three  
151 times, and then dried in a vacuum oven at 60 °C for 4h.

#### 152 **2.5 Preparation of $\text{Fe}_3\text{O}_4@SiO_2@GDN$ microspheres**

153 The as-obtained superparamagnetic  $\text{Fe}_3\text{O}_4@SiO_2$  microspheres (400 mg) were  
154 dispersed in 80.0 mL Tris-HCl buffer (pH 8.21,  $0.1\text{ mol L}^{-1}$ ), followed by the addition  
155 of 3-guanidinopropyl triethoxysilane (1.2 mL, 3.17 mmol) and TEOS (0.6 mL, 2.69



156 mmol). Subsequently, the mixtures were oscillated with  $150 \text{ rpm min}^{-1}$  for 16 h. The  
157 products were collected and washed with deionized water several times to remove the  
158 unreacted monomers. After dried at  $35 \text{ }^\circ\text{C}$  for 24h, the obtained  $\text{Fe}_3\text{O}_4@\text{SiO}_2@\text{GDN}$   
159 microspheres were dried. For comparison, amino group functionalized  
160 superparamagnetic  $\text{Fe}_3\text{O}_4@\text{SiO}_2$  ( $\text{Fe}_3\text{O}_4@\text{SiO}_2@\text{APS}$ ) microspheres were also  
161 prepared under similar condition, except that 3-aminopropyl triethoxysilane  
162 replaced 3-guanidopropyl triethoxysilane as functional monomer.

### 163 **2.6 Recognition of proteins using $\text{Fe}_3\text{O}_4@\text{SiO}_2@\text{GDN}$ microspheres**

164 In a typical experiment,  $\text{Fe}_3\text{O}_4@\text{SiO}_2@\text{GDN}$  microspheres (10.0 mg) were added into  
165 HEPES buffer (2.0 mL, 10mM, pH 6.86) containing the target protein. When the  
166 adsorption reaction was finished, the  $\text{Fe}_3\text{O}_4@\text{SiO}_2@\text{GDN}$  microspheres were  
167 collected from the solution by an external magnetic field, and the protein  
168 concentration of the supernatant was detected. The amount of protein adsorbed onto  
169  $\text{Fe}_3\text{O}_4@\text{SiO}_2@\text{GDN}$  microspheres was calculated from the difference of the  
170 concentration of target protein in the supernatant before and after adsorption. The  
171 adsorption capacity ( $Q$ , mg of protein /g of material) was calculated according to the  
172 following equation:  $Q = (C_0 - C_f)V/W$ , where  $C_0$  (mg/mL) is the initial protein  
173 concentration,  $C_f$  (mg/mL) is the final protein concentration,  $V$  (mL) is the total  
174 volume of the adsorption mixture, and  $W$  (g) is the mass of material.

### 175 **2.7 Capture of intact phosphorylated proteins from standard protein** 176 **mixtures**

177 The superparamagnetic  $\text{Fe}_3\text{O}_4@\text{SiO}_2@\text{GDN}$  microspheres (40.0 mg) were added into  
178 HEPES buffer (40.0 mL, 10 mM pH 6.86) containing a protein mixture (Cyc, Lyz,  
179 BSA, Mb and OVA, or Cyc, BSA and  $\beta$ -Cas), and incubated at  $4 \text{ }^\circ\text{C}$  for 2 h. The  
180 superparamagnetic  $\text{Fe}_3\text{O}_4@\text{SiO}_2@\text{GDN}$  microspheres were collected and washed

181 with 1.0 mL HEPES buffer (pH 6.86). Then 500  $\mu$ L 50 vol % acetonitrile with 1.0  
182 vol % TFA was used to elute the adsorbed proteins twice. The initial solution,  
183 washing and eluent were all analyzed by HPLC.

## 184 **2.8 Capture of phosphopeptides from the mixture of peptides**

185  $\beta$ -Cas (1.0 mg) was first dissolved in 1.0 mL of ammonium bicarbonate solution (50  
186 mM pH 8.0), and then digested with trypsin (enzyme/protein, 1:40 in weight ratio) at  
187 37 °C for 16 h. Tryptic digests were diluted with HEPES (pH 6.86, 10 mM) buffer to  
188 a final concentration of 50 fmol/ $\mu$ L. The resulting material (6.0 mg) was put into the  
189 diluted solution (1.0 mL), and kept for 30 min. The phosphopeptides-loaded  
190 microspheres were collected by an extra magnetic field and washed two times with  
191 2.0 mL of mixture of acetate buffer (100 mM, pH 4.0)/acetonitrile (v/v, 4:1) to  
192 remove non-specific peptides. The bound phosphopeptides were then eluted with 60  
193  $\mu$ L of 50.0% acetonitrile with 1.0% TFA. 2.0  $\mu$ L of the eluent was mixed with 4.0  $\mu$ L  
194 of saturated HCAA, and then 1.0  $\mu$ L of mixture was added to the sample spot.  
195 Samples were analyzed by MALDI-TOF-MS after air drying.

196 In order to construct the complex sample, Cyc was first digested as follow: 1.24 mg of  
197 Cyc was dissolved in ammonium bicarbonate solution (500  $\mu$ L, 50 mM) containing  
198 8 M urea. The solution was kept at 37 °C for 3 h, and then 10  $\mu$ L of DTT (100 mM)  
199 was added. The mixture was kept at 37°C for another 2.0 h, and then 20  $\mu$ L of IAA  
200 (100 mM) was added and incubated for an additional 30 min at room temperature in  
201 the dark. The obtained solution was diluted to 5.0 mL with ammonium bicarbonate  
202 solution (50 mM) to reduce the concentration of urea. Subsequently, the protein was  
203 digested using trypsin (enzyme/protein, 1:40 in weight ratio) at 37 °C for 16 h. The  
204 digested product had a concentration of 20 pmol/ $\mu$ L. 40  $\mu$ L of digested  $\beta$ -cas solution  
205 (1 pmol/ $\mu$ L) was mixed with 200  $\mu$ L digested Cyc solution (20 pmol/ $\mu$ L). The mixture

206 was then diluted with HEPES buffer (pH 6.86, 10 mM) to a total volume of 4.0 mL,  
207 and resulted in a concentration of 10 fmol/ $\mu$ L and 1000 fmol/ $\mu$ L for digested  $\beta$ -Cas  
208 and digested Cys, respectively. The resulting solution (4.0 mL) was mixed with 10.0  
209 mg of Fe<sub>3</sub>O<sub>4</sub>@SiO<sub>2</sub>@GDN for 30 min. The subsequent procedures are as same as that  
210 of phosphopeptide enrichment from  $\beta$ -Cas tryptic digest.

### 211 **2.9 Selective capture of intact phosphorylated proteins from complex samples**

212 Fat was first removed from fresh milk by centrifugation. The obtained nonfat milk  
213 was diluted 120 times with HEPES buffer (pH 6.86, 10 mM). Egg white was first  
214 separated from yolk, and then diluted 150 times with HEPES buffer (pH 6.86, 10  
215 mM). The superparamagnetic Fe<sub>3</sub>O<sub>4</sub>@SiO<sub>2</sub>@GDN microspheres (30.0 mg) were  
216 incubated with 6.0 mL of the diluted nonfat milk or the diluted egg white solution at  
217 4<sup>0</sup>C for 2h. After magnetic collected, the superparamagnetic Fe<sub>3</sub>O<sub>4</sub>@SiO<sub>2</sub>@GDN  
218 microspheres were washed with 1.0 mL HEPES buffer (pH 6.86) twice. Then the  
219 adsorbed proteins were removed from the materials with 1.0 mL 50 vol % acetonitrile  
220 containing 1.0 vol % TFA. The initial diluted samples, supernatant, washing and  
221 eluent were all analyzed by SDS-PAGE.

222 Tissue protein extract from mouse liver was prepared according to a procedure  
223 described in detail elsewhere.<sup>22</sup> Then the extracted liver proteins were precipitated  
224 using cold acetone, and lyophilized to dryness using a lyophilizer. 40.0 mg of liver  
225 proteins were dissolved in 40.0 mL HEPES buffer (pH 6.86, 10 mM, 4 °C ). The  
226 solution was centrifugated at 5000rpm/min for 5 min to remove undissolved  
227 substance. The supernatant was incubated with 35.0 mg of Fe<sub>3</sub>O<sub>4</sub>@SiO<sub>2</sub>@GDN for 30  
228 min at 4 °C. Then the microspheres were washed with 2.0 mL of an acetate buffer

229 (100 mM, pH 4.0) /acetonitrile (v/v, 4:1) twice, and then the bound proteins were  
230 eluted by 200  $\mu$ L of 50.0% acetonitrile with 1.0% TFA. The initial diluted samples,  
231 supernatant, washing and eluent were all analyzed by SDS-PAGE.

### 232 **3. Results and Discussion**

#### 233 **3.1 Preparation and characterization of Fe<sub>3</sub>O<sub>4</sub>@SiO<sub>2</sub>@GDN microspheres**

234 In this study, 3-guanidopropyl triethoxysilane was first synthesized by the reaction of  
235 2-ethyl-2-thiopseudourea hydrobromide with  $\gamma$ -APS in the medium of DMSO and  
236 THF. Monodisperse magnetic Fe<sub>3</sub>O<sub>4</sub> microspheres were prepared by a modified  
237 sol-gel process, and then coated with TEOS. The resulting magnetic Fe<sub>3</sub>O<sub>4</sub>@SiO<sub>2</sub>  
238 particles were further functionalized with a silane mixture containing 3-guanidopropyl  
239 triethoxysilane and TEOS in Tris buffer (pH 8.20), and leading to the formation of a  
240 guanidine-containing silica layer onto the surface of Fe<sub>3</sub>O<sub>4</sub>@SiO<sub>2</sub>. The resulting  
241 Fe<sub>3</sub>O<sub>4</sub>@SiO<sub>2</sub>@GDN microspheres were then employed to capture intact  
242 phosphorylated proteins from complex samples (Figure 1).

243 In order to ensure successful preparation of Fe<sub>3</sub>O<sub>4</sub>@SiO<sub>2</sub>@GDN microspheres, TEM  
244 and SEM were employed to observe the morphology of Fe<sub>3</sub>O<sub>4</sub>@SiO<sub>2</sub> and  
245 Fe<sub>3</sub>O<sub>4</sub>@SiO<sub>2</sub>@GDN microspheres, respectively. From Figure 2a and 2b, we observed  
246 that the core shell Fe<sub>3</sub>O<sub>4</sub>@SiO<sub>2</sub> microspheres with a 200 nm Fe<sub>3</sub>O<sub>4</sub> core were coated  
247 with a silica layer of 8.5nm. A guanidinium-containing silica layer (20 nm) was  
248 formed onto the surface of Fe<sub>3</sub>O<sub>4</sub>@SiO<sub>2</sub> microsphere by further functionalizing with  
249 the mixture of 3-guanidopropyl triethoxysilane and TEOS (Figure 2c and 2d).

250 The surface composition of Fe<sub>3</sub>O<sub>4</sub>@SiO<sub>2</sub>@GDN microsphere was further measured  
251 by XPS. The XPS spectrum of the resulting microspheres showed four distinct  
252 chemical species: nitrogen, carbon, oxygen, and silicon (Figure 3a). In addition, the  
253 characteristic stretching and bending vibration of guanidinium groups at 3430 and

254  $1635\text{ cm}^{-1}$  were clearly observed in the FT-IR spectra of the 3-guanidopropyl  
255 triethoxysilane and  $\text{Fe}_3\text{O}_4@\text{SiO}_2@\text{GDN}$  microspheres (Figure 3b) respectively,  
256 suggesting a large amount of guanidinium groups in the  $\text{Fe}_3\text{O}_4@\text{SiO}_2@\text{GDN}$   
257 microspheres. From the results of TGA (Figure 3c), a weight loss of 27.8% occurred  
258 for  $\text{Fe}_3\text{O}_4@\text{SiO}_2@\text{GDN}$  microsphere, and 7.4% for  $\text{Fe}_3\text{O}_4@\text{SiO}_2$ . The difference can  
259 be attributed to the thermal decomposition of the guanidopropyl groups of  
260  $\text{Fe}_3\text{O}_4@\text{SiO}_2@\text{GDN}$  microsphere. These results suggested that  $\text{Fe}_3\text{O}_4@\text{SiO}_2@\text{GDN}$   
261 microspheres have been successfully fabricated.

262 The magnetization of  $\text{Fe}_3\text{O}_4$  and  $\text{Fe}_3\text{O}_4@\text{SiO}_2@\text{GDN}$  were investigated by using  
263 VSM measurements (Figure 4a). The results indicated that the magnetization of  
264  $\text{Fe}_3\text{O}_4@\text{SiO}_2@\text{GDN}$  microspheres was more than 38 EMU/g. From Figure 4a, we can  
265 conclude that these microspheres are superparamagnetic at room temperature due to  
266 the lack of magnetic hysteresis. In addition, the resulting  $\text{Fe}_3\text{O}_4@\text{SiO}_2@\text{GDN}$   
267 microspheres are well-dispersed in water without visible aggregation (Figure 4b). In  
268 the presence of a magnetic field, however, the microspheres were completely settled  
269 to the bottom of a test bottle in 30 seconds (Figure 4c). This observation proved that  
270 the functionalized magnetic microspheres possessed a high magnetic responsiveness  
271 for use in magnetic separation.

### 272 **3.2 Recognition property of $\text{Fe}_3\text{O}_4@\text{SiO}_2@\text{GDN}$ microspheres**

273 To test the recognition properties of superparamagnetic  $\text{Fe}_3\text{O}_4@\text{SiO}_2@\text{GDN}$   
274 microspheres to phosphorylated proteins, the two classical phosphorylated proteins,  
275  $\beta$ -Cas and OVA, were chosen as model proteins. The materials were incubated with  
276 HEPES buffer (pH 6.86 10 mM) of protein at  $4\text{ }^\circ\text{C}$ . Following collection by an  
277 external magnetic field, the concentration of protein in the supernatant was measured  
278 by UV-vis at 280 nm. The amount of protein adsorbed onto materials was calculated

279 by the difference of concentration of protein in the supernatant before and after  
280 adsorption. From Figure 5a, we observed that capture efficiency decreased with  
281 increasing initial concentration of proteins, and the adsorption amount increased with  
282 increasing initial concentration of proteins and the maximum capacities were achieved  
283 at an initial concentration of  $1.0 \text{ mg mL}^{-1}$ . The adsorption capacities of the material  
284 for OVA and  $\beta$ -Cas were  $78.8 \text{ mg g}^{-1}$  and  $59.6 \text{ mg g}^{-1}$ , respectively. It is worth to note  
285 that both phosphoproteins with significantly different molecular size showed high  
286 adsorption capacity. The superior phosphorylated protein adsorption property of the  
287 guanidine functionalized magnetic microspheres may result from the strong  
288 interaction between guanidine groups of the microspheres and phosphate groups of  
289 the protein.

290 Adsorption kinetics is one of the important parameters for understanding the protein  
291 binding mechanism and determining the potential of materials in practical application.  
292 Thus the adsorption kinetics of  $\text{Fe}_3\text{O}_4@\text{SiO}_2@\text{GDN}$  was also investigated by  
293 changing the adsorption time from 0 to 1440 min and the initial concentration of  
294 proteins were all kept constantly at  $0.5 \text{ mg mL}^{-1}$ . From the time course of binding  
295 (Figure 5b), the adsorption amount increased significantly in the first 60 min, reaching  
296 about 88% of the maximum binding capacity for OVA and 92% for  $\beta$ -Cas. The  
297 binding capacity almost has no change when the incubation time exceeds 120 min.  
298 The results demonstrated that the synthesized  $\text{Fe}_3\text{O}_4@\text{SiO}_2@\text{GDN}$  possessed a fast  
299 adsorption rate.

### 300 **3.3 Recognition Selectivity of $\text{Fe}_3\text{O}_4@\text{SiO}_2@\text{GDN}$ microspheres**

301 The resulting materials have indicated higher binding capacity for chosen  
302 phosphoproteins, however, selectivity is also an important factor for its real  
303 application. Six non-phosphoproteins (including BSA, Try, Mb, Cyc, Hb and Lyz)

304 with different molecular size and pI were chosen as competitors, and the binding of  
305  $\text{Fe}_3\text{O}_4@\text{SiO}_2@\text{GDN}$  microspheres towards these non-phosphoproteins were evaluated  
306 under the condition of  $0.5\text{ mg mL}^{-1}$  of protein. The results indicated that the  
307  $\text{Fe}_3\text{O}_4@\text{SiO}_2@\text{GDN}$  microspheres showed superior recognition ability towards  $\beta$ -Cas  
308 ( $49.5\text{ mg g}^{-1}$ ) and OVA ( $56.7\text{ mg g}^{-1}$ ) (Figure 6). However, the binding amount of the  
309 microspheres towards other non-phosphoproteins was in the range from  $12.7\text{ mg g}^{-1}$   
310 (BSA) to  $1.2\text{ mg g}^{-1}$  (Cyc). Although BSA has a similar pI (4.5) value with OVA,  
311 binding capacity of  $\text{Fe}_3\text{O}_4@\text{SiO}_2@\text{GDN}$  microspheres towards BSA was significantly  
312 lower than that of OVA. Mb and Hb, which are approximately neutral under the test  
313 conditions, also showed lower binding capacities. The results demonstrated that the  
314  $\text{Fe}_3\text{O}_4@\text{SiO}_2@\text{GDN}$  microspheres displayed specific recognition ability to  
315 phosphorylated proteins. In order to further ascertain the role of guanidinium group in  
316 phosphoproteins recognition,  $\text{Fe}_3\text{O}_4$ ,  $\text{Fe}_3\text{O}_4@\text{SiO}_2$  and  $\gamma$ -aminopropyl triethoxysilane  
317 functionalized  $\text{Fe}_3\text{O}_4@\text{SiO}_2$  ( $\text{Fe}_3\text{O}_4@\text{SiO}_2@\text{APS}$ ) were also employed to bind  $\beta$ -Cas  
318 and OVA, respectively. Among the three materials,  $\text{Fe}_3\text{O}_4@\text{SiO}_2$  showed the lowest  
319 binding capacities for  $\beta$ -Cas ( $2.12\text{ mg g}^{-1}$ ) and OVA ( $4.34\text{ mg g}^{-1}$ ), and  $\text{Fe}_3\text{O}_4$   
320 displayed the highest binding capacities for  $\beta$ -Cas ( $16.6\text{ mg g}^{-1}$ ) and OVA ( $8.90\text{ mg}$   
321  $\text{g}^{-1}$ ), which may be attributed to the interaction of unoccupied orbital of iron with the  
322 phosphate group of phosphoprotein. Although there are amine groups on the surface  
323 of  $\text{Fe}_3\text{O}_4@\text{SiO}_2@\text{APS}$ , it still showed lower binding capacities for  $\beta$ -Cas ( $8.9\text{ mg g}^{-1}$ )  
324 and OVA ( $5.70\text{ mg g}^{-1}$ ), respectively. The superior phosphorylated protein adsorption  
325 property of the  $\text{Fe}_3\text{O}_4@\text{SiO}_2@\text{GDN}$  microspheres may result from the strong  
326 interaction between guanidine groups of the microspheres and phosphate groups of  
327 the protein. The results indicated that guanidinium group of  $\text{Fe}_3\text{O}_4@\text{SiO}_2@\text{GDN}$   
328 microspheres played an important role in phosphoproteins recognition.

329 **3.4 Highly specific enrichment of phosphoproteins from standard protein**  
330 **mixtures**

331 Phosphoproteins are usually present at very low concentration in complex biological  
332 samples. Thus, the separation ability of the  $\text{Fe}_3\text{O}_4@\text{SiO}_2@\text{GDN}$  microspheres for  
333 low-concentration proteins was also investigated. Here  $\beta$ -Cas was chosen as  
334 phosphoprotein, and its concentration was kept constant at  $0.01\text{mg mL}^{-1}$ . BSA and  
335 Cyc were chosen as nonphosphoproteins, the concentration for each nonphosphoprotein  
336 was varied in the range of  $0.01\text{mg mL}^{-1}$  to  $1.20\text{ mg mL}^{-1}$ . A series of diluted protein  
337 mixture ( $\beta$ -Cas, Cyc and BSA) were prepared in different mass ratio (phosphoprotein  
338 ( $0.01\text{mg mL}^{-1}$ )/each nonphosphoprotein) at 1:1, 1:20, 1:40 and 1:120 to simulate  
339 complex samples. The initial solution, washing solution and eluted fraction was  
340 detected by HPLC to evaluate the enrichment efficiencies of phosphorylated proteins.  
341 From Figure 7 we can observe that the peaks of BSA and Cyc are apparent in initial  
342 solution, when the mass ratio was beyond 1:20. The peaks of BSA and Cyc are also  
343 observed in washing fraction. The peak of  $\beta$ -Cas, which is undetectable in the initial  
344 solution and washing fraction, is significantly visible in the eluent in all cases. When  
345 the ratio is beyond 1:40, the peak of BSA is also visible in the eluent, however, the  
346 enrichment efficiencies of BSA is less than 5% in all cases. Cyc shows no significant  
347 effect to  $\beta$ -Cas enrichment. It is worth to note that the enrichment efficiencies of  
348  $\beta$ -Cas were beyond 82.6 % and no Cyc was observed in all cases. The separation  
349 ability of the  $\text{Fe}_3\text{O}_4@\text{SiO}_2@\text{GDN}$  microspheres for another classical phosphoprotein,  
350 OVA, was also investigated in the presence of nonphosphoproteins (Lyz, BSA, Mb



351 and Cyc). Protein mixtures (including OVA, Lyz, Mb, Cyc and BSA) with different  
352 mass ratio (phosphoprotein ( $0.01 \text{ mg mL}^{-1}$ )/ each nonphosphoprotein at 1:1, 1:20,  
353 1:40 and 1:120) were obtained by varying the concentration of each  
354 nonphosphoprotein in the range of  $0.01 \text{ mg mL}^{-1}$  to  $1.20 \text{ mg mL}^{-1}$ . Figure 8 showed  
355 the results of the  $\text{Fe}_3\text{O}_4@\text{SiO}_2@\text{GDN}$  microspheres for OVA enrichment from  
356 protein mixtures. When the mass ratio is reached 1:20, the peaks of  
357 nonphosphoproteins are significantly observed in initial solution, and all of them  
358 except BSA are undetected in eluent. OVA could not be observed in initial solution,  
359 and significantly exists in eluent in all cases. The enrichment efficiencies of OVA  
360 were beyond 50%, while Lyz, Cyc and Mb showed no effect to OVA enrichment in  
361 the studied conditions. Although BSA was observed in eluent, the enrichment  
362 efficiencies of BSA are no more than 10% in all cases. These results indicated that the  
363 resulting materials exhibited highly selective binding to phosphoproteins.

### 364 **3.5 Enrichment of phosphopeptides from the mixture of peptides**

365 Selective enrichment of phosphopeptides by the resulting materials was also  
366 investigated. For comparison, the  $\beta$ -Cas digest was directly analyzed by MS. The  
367 obtained spectrum was dominated by non-phosphopeptides, and no phosphopeptide  
368 was observed without the pretreatment procedure (Figure 9a). However, when the  
369 mixture of peptide was treated with  $\text{Fe}_3\text{O}_4@\text{SiO}_2@\text{GDN}$  microspheres, signals of  
370 phosphopeptides could be clearly observed (Figure 9b). In addition, their  
371 dephosphorylated counterparts, which may be formed during the MALDI ionization  
372 process, have also been observed in Figure 9b. The enrichment ability of the resulting

373 material towards phosphopeptides from complex samples were also investigated by a  
374 mimic biological sample, which was constructed by mixing large amounts of tryptic  
375 digests of Cys with the tryptic digests of  $\beta$ -Cas (the molar ratio of Cys to  $\beta$ -Cas is  
376 100:1). The mixture of peptides was analyzed without enrichment; no  
377 phosphopeptides were detected due to the presence of high-abundance  
378 non-phosphopeptides (Figure 9c). After the enrichment, all the three phosphopeptides  
379 could be easily detected with a very clean background in the mass spectrum (Figure  
380 9d). All these results indicated that the resulting materials also showed high  
381 selectivity to phosphopeptides.

### 382 3.6 Highly specific enrichment of phosphoprotein from real biological samples

383 Material capable of enriching phosphoproteins from real complex samples is a  
384 prerequisite for its practical application in proteomic study. Herein, milk, egg white  
385 and tissue protein extract from mouse liver were employed to further examine the  
386 selectivity of  $\text{Fe}_3\text{O}_4@\text{SiO}_2@\text{GDN}$  microspheres in the enrichment of phosphoproteins  
387 from real complex samples. The initial solution, supernatant, washing and eluent were  
388 checked by SDS-PAGE. The obtained gels were stained first with Pro-Q (Figure 10 b,  
389 d and f), which selectively stains phosphoproteins, followed by CBB staining (Figure  
390 10 a, c and e). As shown in Figure 10a and b, more kinds of phosphoproteins were  
391 observed in eluted fraction than in initial diluted milk sample, and eluted fraction has a  
392 much more  $\beta$ -cas than that of initial diluted milk sample. In addition, no protein was  
393 detected in washing solution that indicated no loss of phosphoprotein occurred during  
394 the washing steps. Similar results were also obtained in the enrichment of OVA from

395 egg white. In Figure 10c and d, eluted fraction had relative high concentration of  
396 OVA when compared with the initial diluted egg white mixture. In Figure 10e and f,  
397 there was little signal of phosphoprotein in initial solution, supernatant, and washing  
398 solution. However, many phosphoproteins could be found in eluent solution (Figure  
399 10f). These results indicated the high selectivity of  $\text{Fe}_3\text{O}_4@\text{SiO}_2@\text{GDN}$  microspheres  
400 in enrichment of phosphoproteins from real biological samples. Moreover, the  
401 inherent capability of convenient enrichment by magnetic separation is the great  
402 additional advantage.

#### 403 **4. Conclusions**

404 We have demonstrated for the first time the feasibility of using guanidine  
405 functionalized  $\text{Fe}_3\text{O}_4$  microspheres for high efficient capture of phosphorylated  
406 proteins and peptides in a simple, general, and inexpensive way. The  
407  $\text{Fe}_3\text{O}_4@\text{SiO}_2@\text{GDN}$  microspheres showed the following excellent properties for the  
408 selectively capture of phosphorylated proteins and peptides. 1) The guanidine  
409 functionalized materials are dispersible in water, and can be easily collected from the  
410 mixture just by an external magnetic field. 2) The recognition ability is hardly  
411 affected by pH value of medium (data not shown). 3) The materials display excellent  
412 stability by several adsorption-desorption cycles (binding amount of protein decreased  
413 only 8.5% after six cycles.). 4) The strong specific interaction between guanidine  
414 groups and phosphate groups ensures the guanidine functionalized magnetic  
415 microspheres with high affinity and specificity to different phosphoproteins and  
416 phosphopeptides. With all these features, the guanidine functionalized

417 superparamagnetic microspheres can efficiently and selectively capture low  
418 concentrations of intact phosphorylated proteins and peptides from complex mixtures.  
419 It is also expected that the selective capture is not limited to proteins and peptides, but  
420 can also be extended to phosphate containing biomolecules such as DNA.

421

## 422 **Acknowledgements**

423 This work was supported by the National Natural Science Foundation of China  
424 (Project No.21075089, 31225021 and 21375094), the Ministry of Science and  
425 Technology of China (Project No. 2013AA102202), and the program for Changjiang  
426 Scholars and Innovative Research Team in University (IRT1166).

427

428

## 429 REFERENCES

- 430 1 P. Cohen, The origins of protein phosphorylation, *Nat. Cell. Biol.*, 2002, **4**,  
431 127-130.
- 432 2 N. Dephoure, C. Zhou, J. Villén, S.-A. Beausoleil, C.-E. Bakalarski, S.-J. Elledge  
433 and S.-P. Gygi, A quantitative atlas of mitotic phosphorylation, *Proc. Natl. Acad.*  
434 *Sci. USA.*, 2008, **105**, 10762-10767.
- 435 3 I.-L. Batalha, C.-R. Lowe and A.-C.-A. Roque, Platforms for enrichment of  
436 phosphorylated proteins and peptides in proteomics, *Trends Biotechnol.*, 2012,  
437 **30**, 100-110.
- 438 4 B. Salovska, A. Tichy, M. Rezacova, J. Vavrova and E. Novotna, Enrichment  
439 strategies for phosphoproteomics: state-of-the-art, *Rev. Anal. Chem.*, 2012, **31**,  
440 29-41.
- 441 5 A. Tichy, B. Salovska, P. Rehulka, J. Klimentova, J. Vavrova, J. Stulik and L.  
442 Herychova, Phosphoproteomics: Searching for a needle in a haystack,  
443 *Proteomics*, 2011, **74**, 2786-2797.
- 444 6 M. Lenman, C. Sörensson and E. Andreasson, Enrichment of Phosphoproteins  
445 and Phosphopeptide Derivatization Identify Universal Stress Proteins in Elicitor-  
446 Treated Arabidopsis, *Mol. Plant Microbe Interact.*, 2008, **21**, 1275-1284.
- 447 7 M. Machida, H. Kosako, K. Shirakabe, M. Kobayashi, M. Ushiyama, J. Inagawa,  
448 J. Hirano, T. Nakano, Y. Bando, E. Nishida and S. Hattori, Purification of  
449 phosphoproteins by immobilized metal affinity chromatography and its  
450 application to phosphoproteome analysis, *Febs. J.*, 2007, **274**, 1576-1587.

- 451 8 I.-S. Sheoran, A.-R.-S. Ross, D.-J.-H. Olson and V.-K. Sawhney, Compatibility  
452 of plant protein extraction methods with mass spectrometry for proteome  
453 analysis, *Plant Sci.*, 2009, **176**, 99-104.
- 454 9 R. Krüger, F. Wolschin, W. Weckwerth, J. Bettmer and W.-D. Lehmann, Plant  
455 protein phosphorylation monitored by capillary liquid chromatography-element  
456 mass spectrometry, *Biochem. Biophys. Res. Commun.*, 2007, **355**, 89-96.
- 457 10 Z.-D. Lu, M.-M. Ye, N. Li, W.-W. Zhong and Y.-D. Yin, Self-Assembled TiO<sub>2</sub>  
458 Nanocrystal Clusters for Selective Enrichment of Intact Phosphorylated Proteins,  
459 *Angew. Chem. Int. Ed.*, 2010, **49**, 1862-1866.
- 460 11 A. Dubrovskaja and S. Souchelnytskyi, Efficient enrichment of intact  
461 phosphorylated proteins by modified immobilized metal-affinity chromatography,  
462 *Proteomics*, 2005, **5**, 4678-4683.
- 463 12 G.-C. Adam, E.-J. Sorensen and B.-F. Cravatt, Chemical Strategies for Functional  
464 Proteomics, *Mol. Cell. Proteomics*, 2002, **1**, 781-790.
- 465 13 M.-D. Best, S.-L. Tobey and E.-V. Anslyn, Abiotic guanidinium containing  
466 receptors for anionic species, *Coord. Chem. Rev.*, 2003, **240**, 3-15.
- 467 14 P. Blondeau, M. Segura, R. Pérez-Fernández and J.-D. Mendoza, Molecular  
468 recognition of oxoanions based on guanidinium receptors, *Chem. Soc. Rev.*, 2007,  
469 **36**, 198-210.
- 470 15 D.-W. Christianson and W.-N. Lipscomb, Carboxypeptidase A, *Acc. Chem. Res.*,  
471 1989, **22**, 62-69.

- 472 16 F.-A. Cotton, E.-E.-J. Hazen and M.J. Legg, Staphylococcal nuclease: proposed  
473 mechanism of action based on structure of enzyme-thymidine  
474 3',5'-bisphosphate-calcium ion complex at 1.5-Å resolution, *Proc. Natl. Acad. Sci.*  
475 *USA.*, 1979,**76**, 2551-2556.
- 476 17 E.-E Kim, and H.-W. Wyckoff, Reaction mechanism of alkaline phosphatase  
477 based on crystal structures: Two-metal ion catalysis, *J. Mol. Biol.*, 1991, **218**,  
478 449-464.
- 479 18 A.-S. Woods, and S. Ferré, Amazing Stability of the Arginine-Phosphate  
480 Electrostatic Interaction, *J. Proteome Res.*, 2005, **4**, 1397-1402.
- 481 19 B.-J. Calnan, B. Tidor, S. Biancalana, D. Hudson, and A.-D. Frankel,  
482 Arginine-Mediated RNA Recognition: The Arginine Fork, *Science*, 1991, **252**,  
483 1167-1171.
- 484 20 H. Deng, X.-L. Li, Q. Peng, X. Wang, J.-P. Chen and Y.-D. Li, Monodisperse  
485 Magnetic Single-Crystal Ferrite Microspheres, *Angew. Chem. Int. Ed.*, 2005, **44**,  
486 2782-2785.
- 487 21 X.-W. Kan, Q. Zhao, D.-L. Shao, Z.-R. Geng, Z.-L. Wang and J.-J. Zhu,  
488 Preparation and Recognition Properties of Bovine Hemoglobin Magnetic  
489 Molecularly Imprinted Polymers, *J. Phys. Chem.*, 2010, **114**, 3999-4004.
- 490 22 W.-H. Jin, J. Dai, H. Zhou, Q.C. Xia, H-F Zou and R. Zeng, Phosphoproteome  
491 Analysis of Mouse Liver using Immobilized Metal Affinity Purification and  
492 Linear Ion Trap Mass Spectrometry, *Rapid Commun Mass Spectrom.*, 2004, **18**,  
493 2169–2176.

494 **Figure Legends**

495 **Figure 1** Schematic illustration of the material preparation and phosphoproteins  
496 capture process.

497 **Figure 2** SEM and TEM characterization of  $\text{Fe}_3\text{O}_4@\text{SiO}_2$  and  
498  $\text{Fe}_3\text{O}_4@\text{SiO}_2@\text{GDN}$ , (a), (c) SEM; (b), (d) TEM.

499 **Figure 3** Chemical analysis of  $\text{Fe}_3\text{O}_4@\text{SiO}_2@\text{GDN}$  with XPS, FT-IR, and TGA  
500 techniques. a) XPS spectra of  $\text{Fe}_3\text{O}_4@\text{SiO}_2@\text{GDN}$  Surface; b) FT-IR spectra of  
501 3-guanidopropyl triethoxysilane (dark line) and  $\text{Fe}_3\text{O}_4@\text{SiO}_2@\text{GDN}$  (red line); c)  
502 TGA curves of  $\text{Fe}_3\text{O}_4@\text{SiO}_2$  (dark line) and  $\text{Fe}_3\text{O}_4@\text{SiO}_2@\text{GDN}$  (red line).

503 **Figure 4** a) magnetization curve of magnetic microspheres (dark line) and  
504  $\text{Fe}_3\text{O}_4@\text{SiO}_2@\text{GDN}$  (red line), b) Solvent-dispersivity of the  $\text{Fe}_3\text{O}_4@\text{SiO}_2@\text{GDN}$ ; c)  
505 the collection of the  $\text{Fe}_3\text{O}_4@\text{SiO}_2@\text{GDN}$  microspheres by an external magnetic  
506 field.

507 **Figure 5** a) The binding capacity of  $\beta$ -Cas or OVA on  $\text{Fe}_3\text{O}_4@\text{SiO}_2@\text{GDN}$   
508 microspheres; b) adsorption kinetics of  $\beta$ -Cas or OVA on  $\text{Fe}_3\text{O}_4@\text{SiO}_2@\text{GDN}$   
509 microsphere. Error bars represent the standard deviations,  $n = 3$ . Some error bars are  
510 hidden by point markers.

511 **Figure 6** Recognition of  $\text{Fe}_3\text{O}_4@\text{SiO}_2@\text{GDN}$  towards different proteins. Error  
512 bars represent the standard deviations,  $n = 3$ .

513 **Figure 7** Chromatogram of the protein mixture studied and protein binding  
514 efficiencies; a) 1:1; b) 1:20; c) 1:40; d) 1:120; e) corresponding adsorption  
515 efficiencies for proteins studied. The labels "1", "2", "3" in the chromatograms



516 represent the initial solution, the eluent and washing solution, respectively. Error  
517 bars represent the standard deviations,  $n = 3$ . Some error bars are hidden by point  
518 markers.

519

520 **Figure 8** Chromatogram of the protein mixture studied and protein binding  
521 efficiencies; a) 1:1; b) 1:20; c) 1:40; d) 1:120; e) Corresponding adsorption  
522 efficiencies for proteins studied. The labels “1”, “2”, “3” in the chromatograms  
523 represent the initial solution, the eluent and washing solution, respectively. Error  
524 bars represent the standard deviations,  $n = 3$ . Some error bars are hidden by point  
525 markers.

526 **Figure 9** MALDI mass spectra for selective enrichment of phosphopeptides by  
527  $\text{Fe}_3\text{O}_4@\text{SiO}_2@\text{GDN}$  microspheres. (a) Direct analysis of tryptic digest of  $\beta$ -Cas; (b)  
528 phosphopeptides enriched from tryptic digest of  $\beta$ -Cas; (c) Direct analysis of the  
529 mixture of tryptic digests of  $\beta$ -Cas and Cyc with ratio of 1:100; (d) phosphopeptides  
530 enriched from the mixture of tryptic digests of  $\beta$ -Cas and Cyc with ratio of 1:100. \*  
531 indicates phosphopeptides, ● indicates their dephosphorylated counterparts.

532 **Figure 10** SDS polyacrylamide gel electrophoresis analysis of phosphoproteins  
533 adsorbed onto the materials. S represents supernatant fraction; W represents washing  
534 fraction; E represents eluent; M represents marker proteins (from top to down):  
535  $\beta$ -galactosidase, BSA, OVA, Lactate dehydrogenase, REase Bsp981,  $\beta$ -lactoglobulin,  
536 and Lyz. I represents the initial 120-fold dilution of nonfat milk in a) and b), the  
537 initial 150-fold dilution of egg white in c) and d); and tissue extract protein from  
538 mouse liver in e) and f) respectively.. The proteins were visualized with Coomassie

539 brilliant blue (figure 9a, c and e) and Pro-Q® Diamond phosphoprotein gel staining

540 (figure 9b, d and f), respectively.

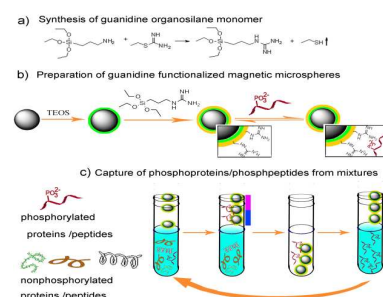
541

542 **TOC**

**Qiliang Deng, Jianhua Wu, Yang Chen,  
Zhiyun Zhang, Yang Wang, Guozhen Fang,  
Shuo Wang\*, Yukui Zhang**

Guanidinium Functionalized  
Superparamagnetic Silica Spheres for  
Selective Enrichment of Phosphopeptides and  
Intact Phosphoproteins from Complex  
Mixtures

Capture of phosphopeptides and phosphoproteins from complex mixtures has been demonstrated based on interaction between phosphate groups and guanidine groups.



543

544

545

546

547

548

549

550

551

552

553

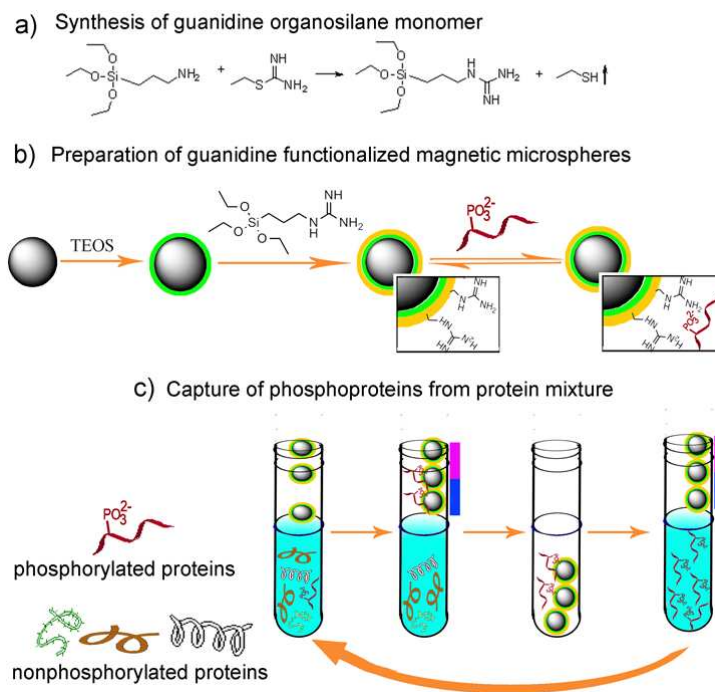
554

555

556

557

558



559

560

561

562

563

564

565

566

567

568

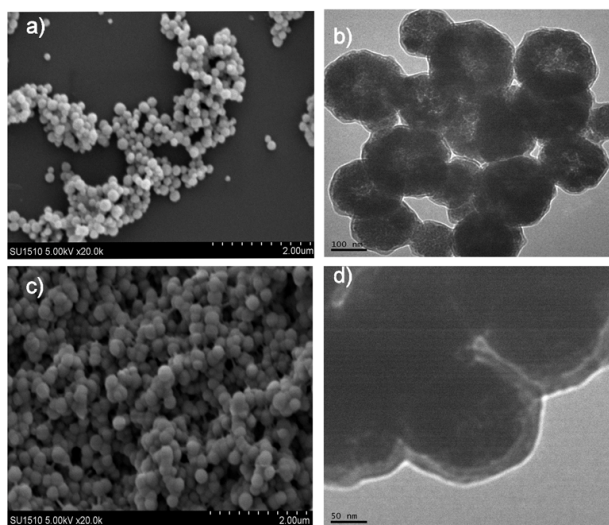
569

570

**Figure 1**

571

572



573

574

**Figure 2**

575

576

577

578

579

580

581

582

583

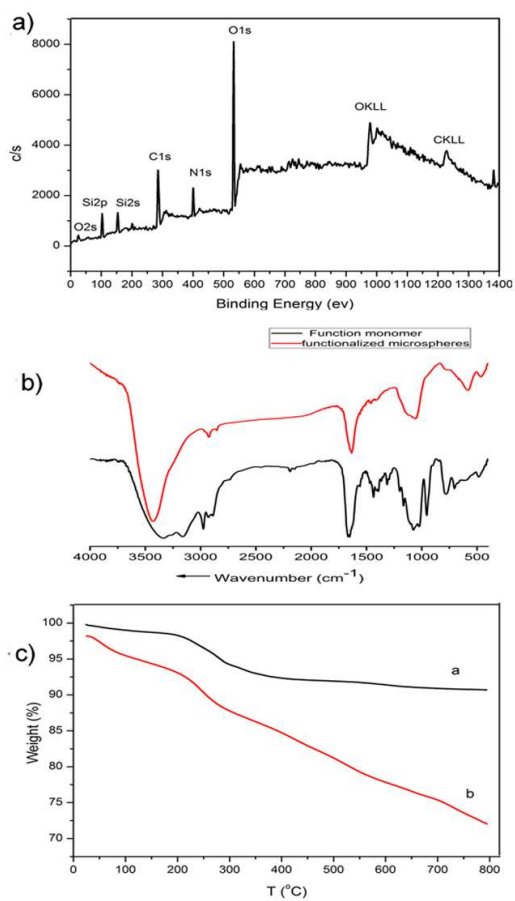
584

585

586

587

588



589

590

591

592

593

594

595

596

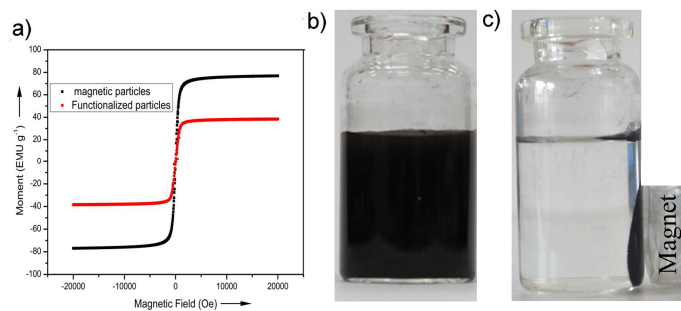
597

598

**Figure 3**

599

600



601

602

**Figure 4**

603

604

605

606

607

608

609

610

611

612

613

614

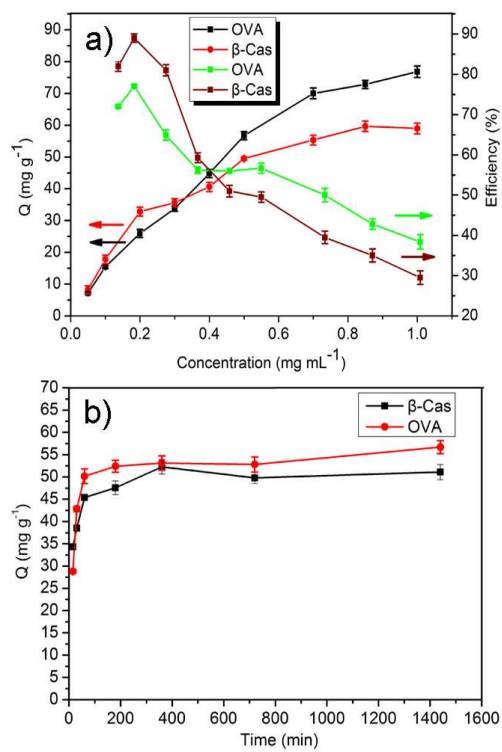
615

616

617

618

619



620

621

622

623

624

625

626

627

628

629

630

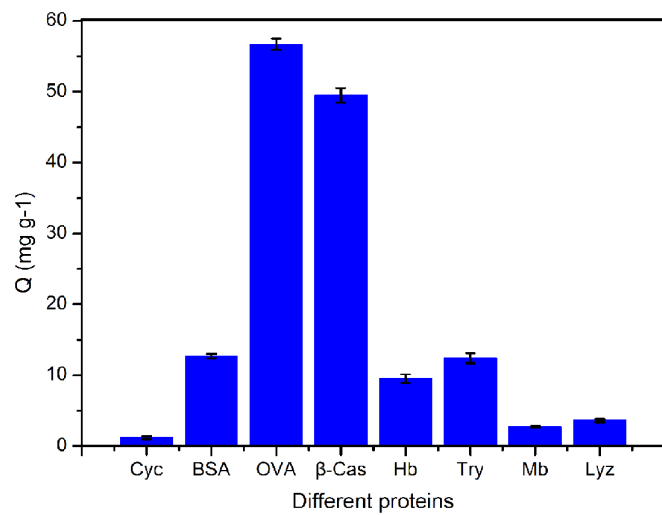
631

**Figure 5**

632

633

634



635

636

**Figure 6**

637

638

639

640

641

642

643

644

645

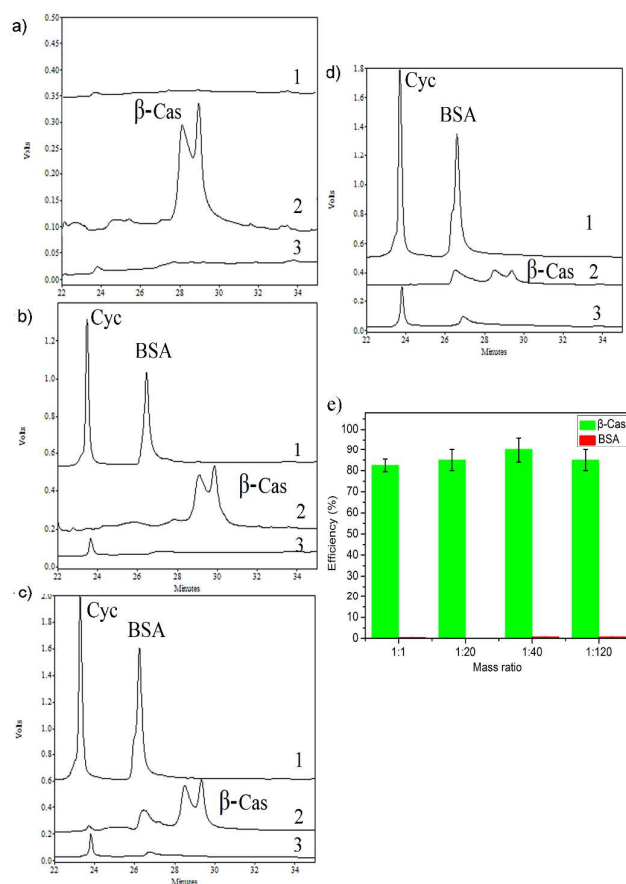
646



647

648

649



650

651

652

653

654

655

656

657

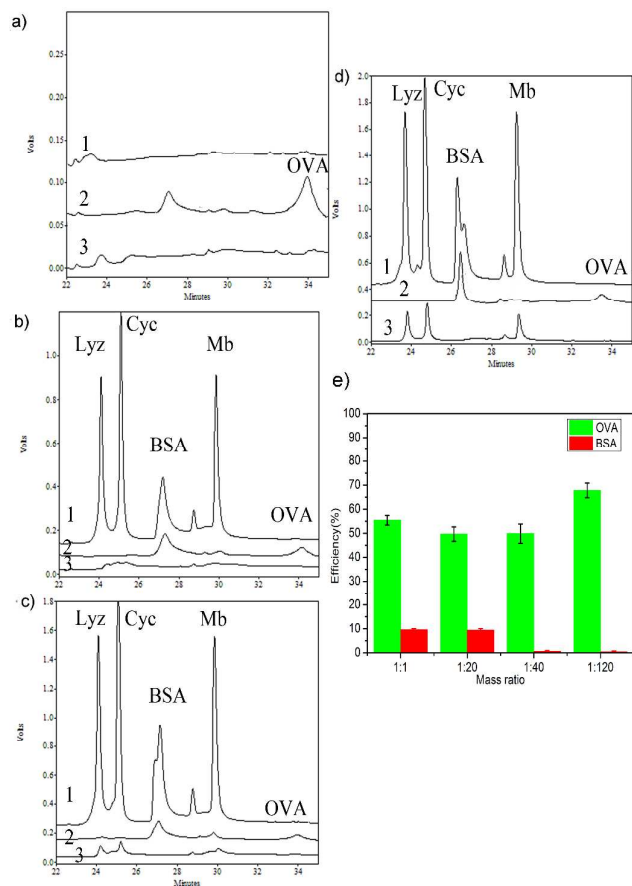
658

Figure 7

659

660

661



662

663

664

665

666

667

668

669

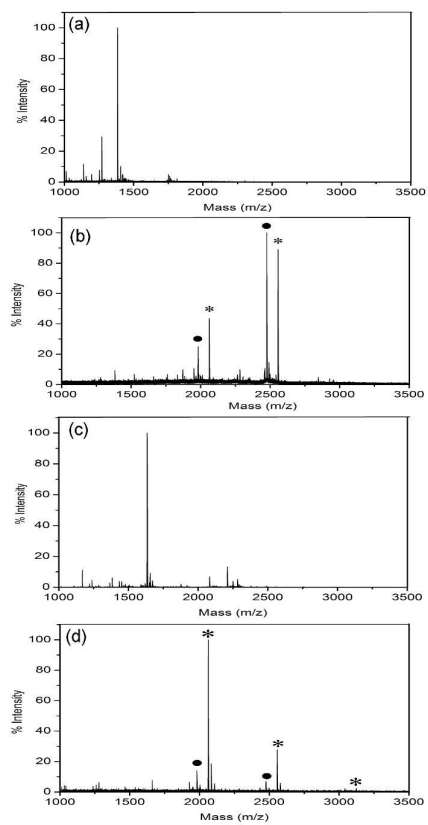
670

Figure 8

671

672

673



674

675

676

677

678

679

680

681

682

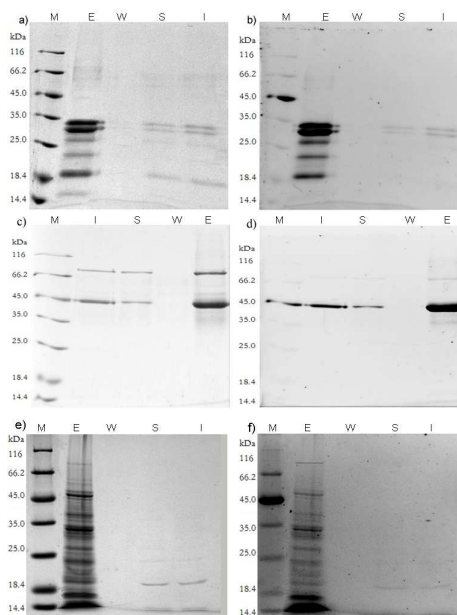
683

**Figure 9**

684

685

686



687

688

689

690

**Figure 10**